Eigenstate symmetries and information transfer in parabolic quantum reflectors

C. Trallero-Giner,[1] V. Lopez-Richard,[2] S. E. Ulloa,[3] and G. E. Marques[2]
[1]*Department of Theoretical Physics, Havana University, Vedado 10400, Havana, Cuba*
[2]*Departamento de Física, Universidade Federal de São Carlos, 13560-905, São Carlos, SP, Brazil*
[3]*Department of Physics and Astronomy and Nanoscale and Quantum Phenomena Institute, Ohio University, Athens, Ohio 457501-2979, USA*

(Received 17 November 2008; revised manuscript received 6 March 2009; published 3 April 2009)

We study the quantum mechanical properties of one of the simplest geometrical elements: a parabolic reflector. We study the quantum propagation problem in a two-dimensional mirror, appropriate for electrons on the surface of metals, providing explicit closed solutions for the particle wave functions and the corresponding energy dispersion. Knowledge of nodal lines and distributions highlights the importance of "silent" and "loud" regions where quantum amplitude would be small or large. We further analyze the effects of quantum focusing and reflection for an initial pulse originating at the focus of the parabolic reflector. We find two propagation fronts that persist at long times and away from the focus of the parabola; the reflected front has higher amplitude and exhibits a nearly flat distribution moving at constant speed along the focal axis, reminiscent of a typical optical mirror wave front.

DOI: 10.1103/PhysRevB.79.153403 PACS number(s): 73.20.−r, 68.37.Ef, 68.49.Jk, 02.60.Lj

The study of quantum coherent propagation in time and/or space is receiving increasing attention in a variety of different experimental systems. The impressive control and manipulation of single and multiple electron spins,[1] or cold atomic condensates near surface deflectors and mirrors,[2] are accompanied by beautiful studies of quantum interference and standing wave patterns on metallic surfaces.[3–5] The availability and continuous development of scanning tunneling microscopes (STM), capable not only of imaging but of manipulating atomic and molecular complexes,[6] have opened up tantalizing possibilities for the study and control of such systems. The fundamental and technological interest in the control, detection, coherence, and tuning of electronic states has resulted in interesting experimental developments, including the recent extraction of phase information from STM images.[7] Indeed, single- and multiple-channel information transfer at the nanometer scale has been proposed on quantum corral systems,[8] which one could envision using in combination with the computation capabilities of molecular-cascade structures,[9] for example.

In this rich context, we present here the development of a rigorous mathematical solution to the eigenstate problem of a quantum parabolic mirror that one could implement on the surface of metals and fully characterize and study utilizing STM techniques. Unlike the discrete spectrum of a quantum corral,[10] the energy spectrum in the space bounded by a parabolic reflector forms a continuum, with peculiar symmetry and degeneracy properties. More interesting, it is clear that this system could become an important element in the transmission of electronic wave packets, and has great potential for additional theoretical and experimental work. As a prominent example of the dynamical features of this geometry, Fig. 1 shows the wave packet propagation obtained for an initially well-localized pulse at the focus of the parabola. The time evolution is easily obtained from the full description of the system, which yields a set of definite-symmetry eigenstates. Utilizing these eigenstates we demonstrate [see Eq. (5) below] that the evolution of the intensity distribution of the initial delta pulse starting at the focus of the reflector has well-defined anterior and posterior wave fronts (Fig. 1). The long-time wave packet develops into a nearly flat wave front that propagates at near constant speed along the focal line, as one could anticipate from the classical light propagation in a parabolic mirror geometry.

The system of interest consists of a two-dimensional (2D) parabolic shaped wall on a substrate (see inset in Fig. 2), with an axis of symmetry which results in wave functions

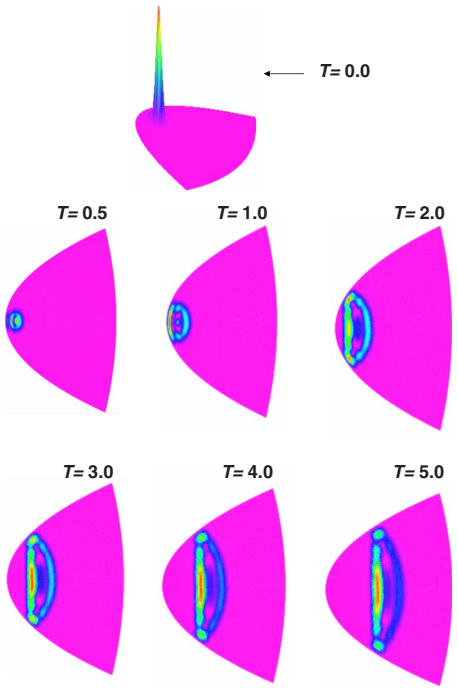

FIG. 1. (Color online) Evolution in a parabolic reflector of an electronic wave packet after a delta emission at the focus at $t=0$ (upper plot). The normalized probability density $|\Psi(\mathbf{r},t)|^2\mu_0^8/2$ is shown at different times T (measured in units of $\tau=\mu_0^4 m/\hbar$, see text below). Notice flat wave front develops at long T traveling at constant speed to the right.

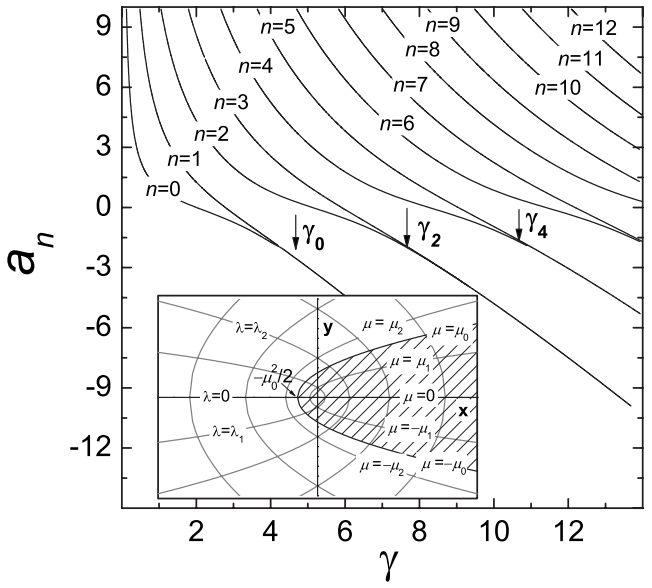

FIG. 2. Quantum reflector eigenvalues, $\gamma=\mu_0^2k/2$, for different reflector quantum numbers a_n. Arrows indicate γ_n values beyond which an accidental degeneracy occurs between adjacent quantum numbers a_n. Inset: Cartesian representation of two-dimensional parabolic coordinates with $|\mu_1|<|\mu_2|<\ldots$ and $\lambda_1<\lambda_2<\ldots$. The domain of the quantum reflector is shaded and defined as the interior problem with boundaries at $\mu=\pm\mu_0$ and $0<\lambda<\infty$.

exhibiting definite (even or odd) inversion symmetry with respect to the confocal axis, as we show below. The system is assumed to be defined on a metallic surface, so that the motion in the direction normal to the substrate is energetically forbidden. The 2D surface states of this metal can be seen as an electron gas, appropriately described by an effective mass with isotropic energy dispersion from the bottom of the band minimum given by $E=\hbar^2k^2/2m$ ($\mathbf{k}$ is the two-dimensional wave vector). The problem is conveniently formulated in parabolic coordinates μ,λ: the quantum reflector is limited to the interior of the parabola, shown in the inset of Fig. 2, with the focus located at the Cartesian coordinate origin $(x,y=0,0)$, and with focal length $\mu_0^2/2$. The 2D quantum problem is described by the Schrödinger equation in parabolic coordinates (for a detailed description see Ref. 10). The wave function on the 2D space confined within the reflector domain must fulfill the (hard wall) boundary conditions, $\Phi(\mu,\lambda)=0$ at $\mu=\pm\mu_0$. This condition leaves unbounded the motion along the λ coordinate; in consequence, the energy spectrum will be continuous and extended from zero to infinity. Meanwhile, motion along the μ coordinate is confined to $|\mu|<\mu_0$, resulting in the appearance of a discrete quantum number, which we label a_n (see below). Hence, for a given value of energy E we have an infinite number of states for different a_n, and an infinitely degenerate spectrum. Since the Hamiltonian is invariant under inversion with respect to the focal axis,[10] i.e., $\mu\rightarrow-\mu$, the wave function $\Phi(\mu,\lambda)$ can be chosen as symmetric or antisymmetric on the μ coordinate. The bounded general solutions for the even (e) and odd (o) states are given by $\Phi_{n,k}^{e(o)}(\mu,\lambda)=N_{n,k}G_{e(o)}(a_n,\mu^2k)F_{e(o)}(a_n,\lambda^2k)$, where

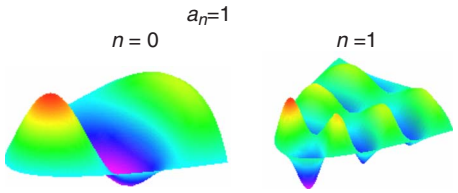

FIG. 3. (Color online) Two calculated wave function maps of the quantum reflector. States with $a_0=1$ and $a_1=1$ ($\gamma\simeq1$ and 2, respectively) are represented.

$$G_{e(o)}=e^{-i\mu^2k/2}\Delta_{e(o)}\mathcal{F}\left(\frac{\Xi_{e(o)}+ia_n}{4},\frac{\Xi_{e(o)}}{2},i\mu^2k\right),\qquad(1)$$

where, $\mathcal{F}(\alpha,\beta,z)$ is the confluent hypergeometric function, $\Delta_{e(o)}=1(\mu\sqrt{k})$, $\Xi_{e(o)}=1(3)$, $N_{n,k}$ is the normalization factor, and a_n is the separation constant determined by the boundary conditions. The functions G and F are related through the equation $F_{e(o)}(a_n,z)=G_{e(o)}(-a_n,z)$. The hard wall boundary conditions are reduced to $G_e(a_{2j},\mu_0^2k)=0$, and $G_o(a_{2j+1},\mu_0^2k)=0$, where the symmetric (antisymmetric) states are characterized by the even (odd) index $n=2j$ $(2j+1)$ with $j=0,1,2\ldots$. These equations provide two sets of independent parametric curves for $a(k)$ for the states as a function of the wave number k. As we stated above, the spectrum is continuous and the functions $\Phi_{n,k}$ have to be normalized in the "k scale." The normalization constant for $\Phi_{n,k}$ can be written in closed analytical form as, $\mu_0N_{n,k}=N_{n,\gamma}$ where

$$N_{n,\gamma}^{(s)}=\frac{(\gamma)^{\pm1/4}\exp\left(-\frac{\pi a_n}{8}\right)}{\mu_0 2^{5/4}\pi}\frac{\left|\Gamma\left(\frac{\Xi_s+ia_n}{4}\right)\right|}{\sqrt{\mathcal{I}_s(\gamma)}},\qquad(2)$$

$\gamma=\mu_0^2k/2$ is the dimensionless wave number, $s=e$, o, and

$$\mathcal{I}_s=\int_0^1\xi^{8(1-\Xi_s)}\left|\mathcal{F}\left(\frac{\Xi_s+ia_n}{4},\frac{\Xi_s}{2},i2\gamma\xi^2\right)\right|^2d\xi.\qquad(3)$$

Figure 2 shows the variation in the first 13 a_n eigenvalues as function of the dimensionless wave number $\gamma=\mu_0^2k/2$. It is important to remark that the results in Fig. 2 present the *general* solution for any γ (as it is scaled in terms of μ_0). It can be seen that a_n decreases monotonically as γ increases, and that $\lim_{\gamma\rightarrow0}a_n=\infty$. Notice that, as mentioned before, the spectrum of the system is infinitely degenerate at a given value of the energy E (γ fixed), i.e., there are infinite eigenstates with different values of a_n for the same γ value. Using the properties of the confluent hypergeometric function $\mathcal{F}(\alpha,\beta,z)$, and its asymptotic behavior for $z\rightarrow\infty$, it is possible to show that $\lim_{\gamma\rightarrow\infty}a_n=-\infty$, $\forall n$, and $\lim_{\gamma\rightarrow\infty}(a_{2j}-a_{2j+1})=0$, $j=0,1,2\ldots$. Figure 2 indicates the latter characteristic of the spectrum, the accidental degeneracy for $\gamma\rightarrow\infty$ of consecutive a_n levels with different parity ($n=2j$ and $n=2j+1$). The minimal value of γ beyond which $a_{2n}\approx a_{2n+1}$, γ_n, depends on the two levels under consideration; higher values of n result in larger values of γ_n. Different parity eigenfunctions are shown in Fig. 3 for different γ values. It is clear that the pattern of nodes and antinodes

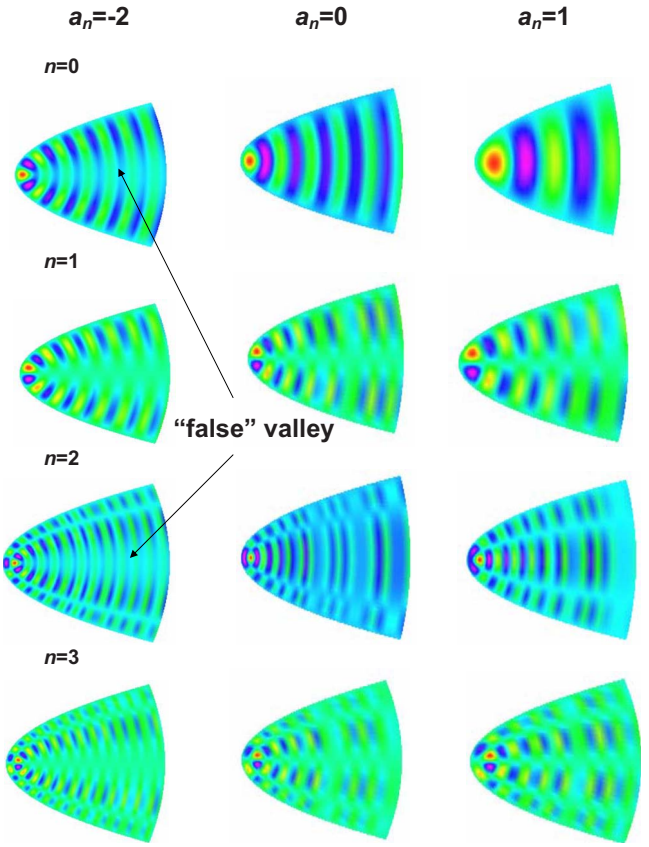

FIG. 4. (Color online) Contour plots of wave function $\Phi_{n,k}(\mu,\lambda)$ for different values of the quantum number a_n. States with even (odd) n are symmetric (antisymmetric) under reflection with respect to the focal line. Low-amplitude false valleys in even states for $a_n=-2$ are indicated by arrows.

changes for different value of the parameter a_n.

Figure 4 shows contour plots for the eigenfunctions $\Phi_{n,k}(\mu,\lambda)$ for $n=0$, 1, 2, 3, for three different values of the parameter a_n. It is interesting that the wave function maps display a fanlike pattern on both sides of the focal axis. Notice that higher n values for $a_n=$const result in larger number of nodes and antinodes along lines of constant μ (as γ or k increase with n as well and the state wavelength gets smaller). In contrast, increasing the value of a_n for a given n results in fewer nodal lines, as k (or γ) is smaller, and the wavelength is larger. Note that the valleys along $\lambda=$const curves arise from the condition $F_{e(o)}(a_n,\lambda^2 k)=0$. The parity of the states, as defined by the index n, can be clearly identified in the reflection symmetry of the nodal peaks and valleys with respect to the focal axis. Every odd state displays a node at $\mu=0$ that coincides with the focal axis for positive values of the Cartesian coordinate x, while for even states evidently, $\Phi^e_{n,k}(0,0)\neq 0$.

There is an interesting effect of "mimicry" between even and odd states for high γ values. As noted in Fig. 2, adjacent levels $n=2j$ and $n=2j+1$ show degeneracy for large γ (or energy), which is reflected in the topology of the wave function. In Fig. 4, one can see that the states with $a_n=-2$ for $n=0$ and 2 acquire a profile that resembles the states $n=1$ and 3, respectively. In fact, all even states develop an apparent valley at the focal line, when the parameter a decreases toward more negative values ($\gamma\to\infty$). This extra valley is in fact a "false" valley, as indicated in Fig. 4, with only a local minimum at $\mu=0$. To clarify the nature of these valleys, the evolution of the wave function with a_n is displayed in Fig. 5. We plot the probability density profile characterized by the even, $|G_e(a_0,\mu^2 k)|^2$, and odd, $|G_o(a_1,\mu^2 k)|^2$, function characterizing the wave function profiles at $\lambda=$const. At $a_0=-1$ the probability density $|G_e(a_0,\mu^2 k)|^2$ shows a profile qualitatively similar to $|G_o(a_1,\mu^2 k)|^2$ (displayed in the inset), although the amplitude on the focal line ($\mu=0$) is nonzero for G_e. In fact, one can verify that the wave function $\Phi^e_{n,k}(0,0)=N^e_{n,k}$ decreases as the energy parameter γ grows [see Eq. (2)], explaining the appearance of the relatively low-amplitude "false" valley associated with the quasidegeneracy reported in Fig. 2.

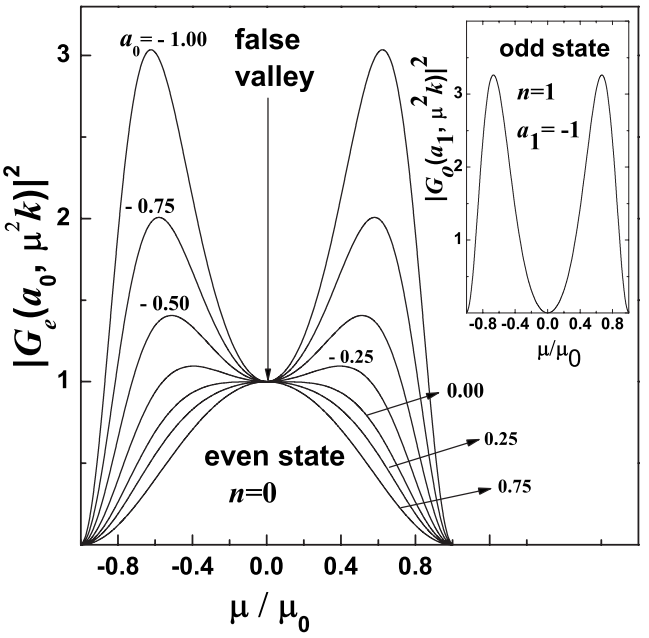

FIG. 5. Profile of $[G_e(a_0,\mu^2 k)]^2$ for various values of the parameter a_0 in the range $[-1,0.75]$. In the inset, the profile of the odd wave function for $a_1=-1$.

The quantum mechanical properties of the parabolic reflectors have potential applications in the control of electronic pulse propagation in these systems. Let us consider the particle "emission" of a well-localized pulse at the focus of the parabola at $t=0$. Hence, the particle wave function presents the form $\Psi(r,0)=\delta(\mathbf{r})$, and the quantum mechanical state evolves in time according to

$$\Psi(\mathbf{r},t)=\sum_n \int g_{n,k}\Phi_{n,k}(\lambda,\mu)\exp\left(-i\frac{E_k t}{\hbar}\right)dk, \qquad (4)$$

where $g_{n,k}$ is the weight function defined by the initial condition. Using the relation $\delta(\mathbf{r})|D(\frac{x,y}{\lambda,\mu})|=\delta(\lambda)\delta(\mu)$, where $|D(\frac{x,y}{\lambda,\mu})|$ is the Jacobian of the transformation to parabolic coordinates, on can write the time dependence of the dimensionless probability density of the emitted pulse as

$$|\Psi(\mathbf{r},t)|^2\frac{\mu_0^8}{2}=\left|\sum_j\int_0^\infty (N_{2j,\gamma}^e)^2F_e\left(a_{2j},2\gamma\left(\frac{\lambda}{\mu_0}\right)^2\right)G_e\left(a_{2j},2\gamma\left(\frac{\mu}{\mu_0}\right)^2\right)\exp(-i\gamma^2T)d\gamma\right|^2, \quad (5)$$

with $T=t/\tau$ and $\tau=\mu_0^4m/\hbar$ being the unit of time.

Figure 1 depicts the time dependence of the probability density $|\Psi(\mathbf{r},t)|^2$. A scale of the intensity distribution at $T=0$ is given in the upper panel of the figure. One can clearly see a spreading wave with two well-defined fronts, anterior, and posterior. Soon after the initial pulse, $T<0.5$, the pulse spreads nearly circularly, as one would expect of an unbound geometry. As the propagating front is reflected by the mirror, $T\simeq 1$, anterior and posterior fronts are located to the right and to the left of the focus of the reflector. The posterior front is strongly distorted by the boundary of the reflector and it starts to reverse its motion. At $T=2$ the posterior front has completely reversed its direction and continues moving to the right in the figure. The anterior front corresponds essentially to an outgoing scattering wave in 2D, which has smaller amplitude as it spreads on the domain surface defined by the parabolic reflector. The shape of this front resembles a confocal parabola and is well defined at each time T by the equation $\lambda=$const. (where the constant increases with T). Notice that for longer $T(\gtrsim 4)$, the anterior front has most of the intensity and shows an essentially flat profile perpendicular to the focal line. This wave front moves with nearly constant speed, and it is reminiscent of the front that one would expect propagating in a classical mirror (although a strong modulation along the front is evident, arising from the quantum nature of this "beam"). We should notice that the time reversibility of the Schrödinger equation guarantees that an incident flat wave front parallel to the focal axis will be reflected into the focus. These properties may find interesting uses in pulse control and measurement.[8]

In summary, we have studied a parabolic quantum reflector as a possible tool for the propagation of wave packets and carefully characterized its eigenstates. The propagation of a particle in a two-dimensional substrate near the parabolic mirror involves "silent" zones with very small probability amplitude, identified with nodal lines on the eigenstates. The propagation of an incoming wave packet with general characteristics moving on the surface can be formulated in terms of the eigenstates introduced here, in order to describe the scattering process in this quantum parabolic reflector. The extent to which this system can be exploited for recording or transmission information is greatly facilitated by STM developments on imaging and manipulation. Although mirrors in those systems are not the perfect reflectors we assume, our analytical solutions provide valuable direct insights that can be further refined by numerical methods when realistic mirrors are studied. We are enthusiastic about future developments in these systems.

The authors acknowledge financial support from Brazilian agencies FAPESP and CNPq. G.E.M. and C.T-G. are grateful to the Visiting Scholar Program of the ICTP/Trieste. S.E.U. acknowledges support of NSF-DMR Grant No. 0710581.

[1] S. A. Wolf, D. D. Awschalom, R. A. Buhrman, J. M. Daughton, S. von Molnár, M. L. Roukes, A. Y. Chtchelkanova, and D. M. Treger, Science **294**, 1488 (2001).
[2] A. E. Leanhardt, Y. Shin, A. P. Chikkatur, D. Kielpinski, W. Ketterle, and D. E. Pritchard, Phys. Rev. Lett. **90**, 100404 (2003).
[3] D. M. Eigler and E. K. Schweizer, Nature (London) **344**, 524 (1990).
[4] J. A. Stroscio and D. M. Eigler, Science **254**, 1319 (1991).
[5] P. Zeppenfeld, C. P. Lutz, and D. M. Eigler, Ultramicroscopy **42-44**, 128 (1992).
[6] S.-W. Hla, J. Vac. Sci. Technol. B **23**, 1351 (2005).
[7] C. R. Moon, L. S. Mattos, B. K. Foster, G. Zeltzer, W. Ko, and H. C. Manoharan, Science **319**, 782 (2008).
[8] D. M. Eigler, C. P. Lutz, M. F. Crommie, H. C. Manoharan, A. J. Heinrich, and J. A. Gupta, Philos. Trans. R. Soc. London, Ser. A **362**, 1135 (2004).
[9] A. J. Heinrich, C. P. Lutz, J. A. Gupta, and D. M. Eigler, Science **298**, 1381 (2002).
[10] C. Trallero-Giner, S. E. Ulloa, and V. López-Richard, Phys. Rev. B **69**, 115423 (2004).